Neuropsychopharmacology

ARTICLE

Altered network connectivity predicts response to cognitive-behavioral therapy in pediatric obsessive–compulsive disorder

Marilyn Cyr[1,2], David Pagliaccio[1,2], Paula Yanes-Lukin[1,2], Martine Fontaine[1,2], Moira A. Rynn[3] and Rachel Marsh[1,2]

Obsessive–compulsive disorder (OCD) is commonly associated with alterations in cortico-striato-thalamo-cortical brain networks. Yet, recent investigations of large-scale brain networks suggest that more diffuse alterations in brain connectivity may underlie its pathophysiology. Few studies have assessed functional connectivity within or between networks across the whole brain in pediatric OCD or how patterns of connectivity associate with treatment response. Resting-state functional magnetic resonance imaging scans were acquired from 25 unmedicated, treatment-naive children and adolescents with OCD (12.8 ± 2.9 years) and 23 matched healthy control (HC) participants (11.0 ± 3.3 years) before participants with OCD completed a course of cognitive-behavioral therapy (CBT). Participants were re-scanned after 12–16 weeks. Whole-brain connectomic analyses were conducted to assess baseline group differences and group-by-time interactions, corrected for multiple comparisons. Relationships between functional connectivity and OCD symptoms pre- and post-CBT were examined using longitudinal cross-lagged panel modeling. Reduced connectivity in OCD relative to HC participants was detected between default mode and task-positive network regions. Greater (less altered) connectivity between left angular gyrus and left frontal pole predicted better response to CBT in the OCD group. Altered connectivity between task-positive and task-negative networks in pediatric OCD may contribute to the impaired control over intrusive thoughts early in the illness. This is the first study to show that altered connectivity between large-scale network regions may predict response to CBT in pediatric OCD, highlighting the clinical relevance of these networks as potential circuit-based targets for the development of novel treatments.

Neuropsychopharmacology (2020) 45:1232–1240; https://doi.org/10.1038/s41386-020-0613-3

INTRODUCTION

Obsessive–compulsive disorder (OCD) is a disabling neuropsychiatric condition characterized by intrusive thoughts (obsessions) and repetitive, ritualistic behaviors (compulsions). Neuroimaging studies of OCD commonly identify structural and functional alterations in cortico-striato-thalamo-cortical (CSTC) brain circuits [1–11]. However, emerging evidence suggest that dysfunction in more diffuse brain networks (e.g., frontoparietal (FPN) and default mode (DMN) networks) may underlie OCD [11–19]. Few studies have assessed functional connectivity within or between such networks in pediatric OCD [20, 21] and none have assessed associations with treatment response. Cognitive-behavioral therapy (CBT) is an effective, first-line treatment for OCD [22–25] that shows better response than pharmacotherapy in pediatric OCD [26–28]. Nevertheless, treatment-resistant symptoms often remain in many patients following either type of treatment [29–32], pointing to the importance of identifying reliable biologically based predictors of response to inform clinical decisions and develop personalized treatments tailored to individual patients (i.e., precision medicine). Resting-state functional magnetic resonance imaging (rs-fMRI) is used to investigate network dynamics in normative and psychiatric populations and can identify biological predictors of clinical outcomes. Herein, we used longitudinal rs-fMRI data from children and adolescents with OCD to identify alterations in large-scale functional networks and characterize connectivity-symptom changes pre- and post-CBT. Such knowledge may ultimately improve treatment selection and foster the development of novel treatments that target brain networks more effectively.

The prevailing neurobiological model of OCD proposes that obsessive–compulsive symptoms arise from altered functioning of the CSTC circuits that support the capacity to engage control over obsessions and urges to perform rituals [33–35]. Indeed, structural and task-based fMRI data implicate OCD-related dysfunctions mainly in fronto-striatal portions of CSTC circuitry [5, 36–46]. Rs-fMRI data also suggest abnormalities in CSTC connectivity, albeit inconsistently, with findings of both hypo- [3, 8] and hyper-connectivity [2, 6, 7]. Other models suggest impairments in large-scale brain networks that extend beyond CSTC circuits, such as altered connectivity within and between FPN, salience, cingulo-opercular, dorsal and ventral attention, and DMN networks [13, 14, 47].

Discrepancies among previous rs-fMRI findings are likely owing to inconsistencies in methods and sample characteristics. For example, studies vary in their use of hypothesis-driven, seed-based connectivity versus hypothesis-free, data-driven analyses. Findings of altered CSTC connectivity stem primarily from seed-based analyses [2, 3, 6, 8], whereas large-scale network findings

[1]Division of Child and Adolescent Psychiatry, New York State Psychiatric Institute, New York, NY, USA; [2]Department of Psychiatry, Vagelos College of Physicians and Surgeons, Columbia University, New York, NY, USA and [3]Department of Psychiatry & Behavioral Sciences, Duke University School of Medicine, Durham, NC, USA
Correspondence: Marilyn Cyr (marilyn.cyr@nyspi.columbia.edu)
These authors contributed equally: Moira A. Rynn and Rachel Marsh.

Received: 12 July 2019 Revised: 21 November 2019 Accepted: 8 January 2020
Published online: 17 January 2020

stem from data-driven whole-brain connectomic approaches [7, 12, 15, 18, 20, 48–55]. Among such approaches, the examination of pairwise associations (i.e., edges) between regions (i.e., nodes) across the entire brain matrix (i.e., the connectome), revealed disturbances in network connectivity in adults with OCD [7, 15, 18, 49, 54, 55]. Only one cross-sectional study used such an approach in pediatric OCD, pointing to less-efficient information transfer and differently organized networks in OCD [20].

In adults with OCD, CBT is associated with changes in multiple brain networks, including, but not restricted to CSTC regions [52]. Baseline connectivity and pre- to post-CBT changes in connectivity are associated with post-CBT symptoms and pre- to post-CBT changes in symptoms [48, 49, 52, 53]. Similar results exist from task-based fMRI studies [31, 56–59]. Univariate analyses such as those used in such prior studies do not permit testing the directionality of relationships between brain measures (i.e., connectivity or activity) and symptoms, thereby precluding inferences about causality [60–62]. Cross-lagged panel modeling, a multivariate approach based on structural equation modeling, can be used to disentangle whether pre-treatment functional connectivity predicts CBT-related changes in OCD symptoms, whether pre-treatment symptom severity predicts changes in functional connectivity, or both (i.e., transactional relationships). This approach allows us to simultaneously test relationships between variables over time while controlling for their cross-sectional association and for the stability of each individual variable across time points. Cross-lagged associations provide a conservative test about the proportion of change in one variable (e.g., OCD symptoms) that is uniquely the result of the other variable (e.g., functional connectivity at baseline), thereby supporting inference about directionality of relationships [63–65].

Herein, we used a data-driven whole-brain connectomic approach to examine the functional connectivity between regions of canonical functional networks [66, 67] in a sample of treatment-naive children and adolescents with OCD. We also used cross-lagged panel modeling to examine relationships between connectivity and OCD symptoms pre- and post-CBT, allowing us to identify and disentangle directional effects. We hypothesized that functional connectivity would be altered between network regions that extend beyond CSTC circuits in pediatric OCD participants and that these alterations would normalize following CBT. We also predicted that less-altered connectivity at baseline would predict better treatment response. Given the scarcity of prior rs-fMRI studies in pediatric OCD and inconsistencies in adult OCD literature, we did not formulate specific hypotheses about the specific networks/regions in which connectivity would be altered, or the direction (i.e., hyper- versus hypo-connected) of such alterations.

METHODS

Participants

Participants were 55 unmedicated and treatment-naive children and adolescents (age 7–18 years), including 28 patients with a primary diagnosis of OCD and 27 matched healthy controls (HC), group-matched for age, sex, race, and ethnicity (CONSORT flowchart in Figure S1). Participants were recruited through New York City area clinics, local, online, and radio advertisements. All participants provided informed assent and their caregiver provided informed consent. The study was approved by the Institutional Review Board at the New York State Psychiatric Institute (NYSPI) where the study was conducted between 2014 and 2017.

At baseline, a structured diagnostic interview, the Anxiety Disorders Interview Schedule for Children (ADIS) adapted for DSM-IV, child and parent versions [68], as well as the Wechsler Abbreviated Scale of Intelligence (WASI) [69] were delivered to all participants. Participants with OCD were also administered the Children's Yale-Brown Obsessive–Compulsive Scale (CY-BOCS), present, and lifetime version [70, 71] to assess OCD symptom severity, as well as the Clinical Global Impressions (CGI) Severity of Illness and Improvement Scale [72] to assess global OCD symptom impression, at baseline, mid-, and end of treatment (see below). OCD patients were included if they met diagnostic criteria for OCD and had clinically significant symptoms (i.e., CY-BOCS > 16) at baseline. Other anxiety disorders (i.e., generalized anxiety disorder, panic disorder, social anxiety disorder, specific phobia, and separation anxiety) were only permitted in the OCD group if OCD was the primary diagnosis. Participants with a history of neurological disorders, past seizures, head trauma with loss of consciousness, mental retardation (i.e., WASI IQ < 80), pervasive developmental disorder, tic disorder, or current psychiatric diagnoses (other than OCD and anxiety in the patients) were excluded. HCs had no lifetime psychiatric diagnoses. Participants were re-scanned 12–16 weeks following their baseline assessment.

CBT treatment

Following baseline assessment, patients with OCD underwent a course of manualized CBT with exposure and response prevention adapted for pediatric OCD [73] delivered by a licensed clinical psychologist or advanced supervised graduate student in clinical psychology at the NYSPI. CBT treatment consisted of 12–16 h-long sessions. In exceptional cases of no clinical improvement after six treatment sessions, as determined by the therapist and study team psychiatrist, complementary pharmacological treatment was offered. See supplementary information for details.

Participant characteristics and treatment outcome analyses

Using IBM SPSS (v.23), group differences in participant demographics were assessed at baseline and follow-up using independent *t* tests for continuous variables and chi-squared tests for categorical variables. A paired *t* test assessed CY-BOCS score decline pre- to post-treatment in the OCD patients.

MRI acquisition

MRI data were collected using a GE Signa 3 Tesla MR750 scanner (Milwaukee, WI), equipped with a 32-channel head coil (Nova), using a scanning protocol adapted from the Human Connectome Project (HCP) protocols [74]. T2-weighted localizing sagittal images (2D) were acquired used to position the axial functional images parallel to anterior commissure-posterior commissure line. The following images were acquired: (1) two high-resolution T1-weighted BRAVO structural images (field of view = 240 mm, flip angle = 12°, 0.8 mm isotropic voxels, 224 slices) and a high-resolution T2-weighted image (TR = 2500 msec, TE = maximum, field of view = 256 mm, flip angle = 12°, 0.8 mm isotropic voxels, 224 slices); (2) two short spin echo, specifically echo planar imaging (EPI) sequences (TR = 5200 msec, TE = 25 msec, field of view = 192 mm, 2 mm isotropic voxels, 72 slices with no gaps) with opposite phase encoding (posterior-anterior vs. anterior-posterior) directions to measure the B0 field for EPI distortion correction; and (3) functional multi-band EPI T2*-weighted images (TR = 850 msec, TE = 25 msec, flip angle = 60°, multi-band factor = 6, field of view = 192 mm, 2 mm isotropic voxels, 66 slices with interleaved acquisition and no gaps, 7 min 42 sec, 544 volumes). Participants were instructed to stay still and keep their eyes open while viewing a fixation cross.

FMRI processing

Twelve frames of scanner calibration data, reconstructed as two EPI volumes, were discarded prior to preprocessing. Six additional EPI volumes were discarded as the scanner reached steady state. The HCP preprocessing pipelines [75] v.3.4 were

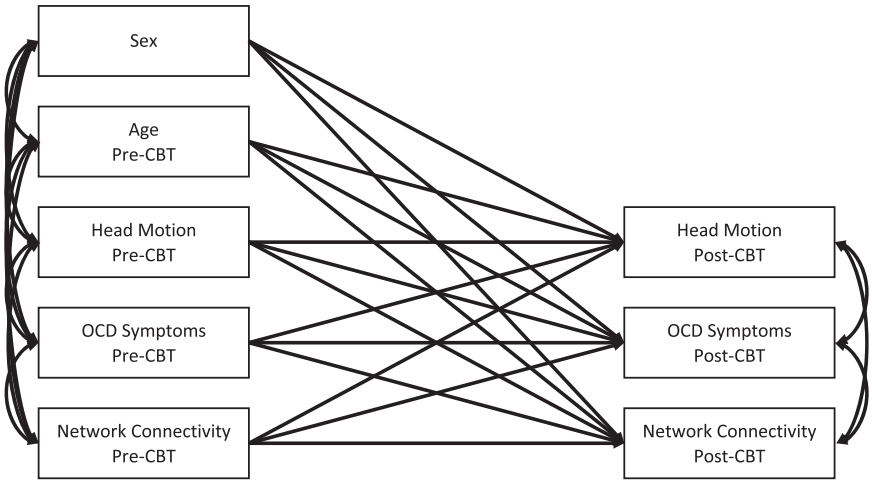

Fig. 1 Schematic of the initial path models relating functional connectivity and obsessive–compulsive disorder (OCD) symptoms before and after cognitive-behavioral therapy (CBT) treatment. Covariances on endogenous variables refer to covariances on error terms of those variables.

used to preprocess all imaging data. In brief, this included gradient unwarping, motion correction, field map-based EPI distortion correction, brain-boundary-based registration of EPI to structural T1-weighted scan, non-linear (FNIRT) registration into MNI152 space, and grand-mean intensity normalization. After this "minimal preprocessing", all analyses were performed in the "grayordinate" space output of the pipeline ("91k" CIFTI format: 91,282 grayordinates, 32,492 per cortical hemisphere and 29,298 subcortical), which combines cortical surface and subcortical volume representations. The surface and subcortical volume data were smoothed with a 4 mm Gaussian kernel using the Workbench software (http://www.humanconnectome.org/software/connectome-workbench) developed by the HCP (wb_command -cifti-smoothing). Additional processing was run in MATLAB R2016a (Mathworks, Natick, MA). Using commands from Analysis of Functional NeuroImages (AFNI; http://afni.nimh.nih.gov/) and FMRIB Software Library (FSL; http://fsl.fmrib.ox.ac.uk/fsl/fslwiki/) software, BOLD signal was demeaned and detrended (AFNI 3dDetrend), despiked (AFNI 3dDespike -localedit), and bandpass filtered (FSL fslmaths 0.01–0.08 Hz). Nuisance regression of 24 motion parameters (bandpass filtered) and average global gray signal was performed. Motion censoring (Power et al., 2012) based on framewise displacement (FD; > 0.2 mm) and DVARS (z score > 3) was also performed.

Whole-brain connectome-level analyses

We conducted resting-state analyses on 333 cortical surface [66] and 19 subcortical [76] parcellated regions, computing rs-fMRI connectivity-strength indices using Fisher Z-Transformation of the pairwise Pearson correlation coefficients between each region. Edge-wise functional connectivity analyses were then conducted whole-brain across the resulting matrix comprised of 352 nodes and 123,904 edges. Analyses examining group differences and group-by-time interactions were adjusted for age at the time of scanning, sex, and head motion (mean FD) and conducted using the Network-Based Statistics Toolbox (v.1.2) [77]. Both false discovery rate (FDR) and network-based statistics (NBS) methods were employed to control for type I error, using a statistical threshold $p = 0.05$ and 20,000 permutations. FDR tests the null hypothesis at the individual connection level and is more sensitive to focal effects, whereas NBS tests the null hypothesis at the network level based on family-wise error and is more sensitive to distributed network effects. For significant findings that converged across these two correction methods, connectivity strengths were extracted from the matrix and used in subsequent analyses to limit the number of statistical tests performed.

Cross-lagged panel modeling

Cross-lagged panel models were constructed using IBM SPSS Amos (v.23) to test for directional ("causal") relationships between OCD symptoms and functional connectivity pre- to post-CBT in the OCD patients. These models provide estimates of the extent to which a variable pre-CBT (e.g., connectivity) predicts another variable post-CBT (e.g., CY-BOCS), over and above the variability attributable to scores of that second variable (e.g., CY-BOCS) pre-CBT [78]. Thus, by controlling for the effects of each variable pre-CBT on the same variable post-CBT, pre-CBT variables then predict the residual, or change in that variable from pre- to post-CBT. CY-BOCS total scores at each time point were used as the OCD symptoms measure.

The initial model, depicted in Fig. 1, adjusted for age, sex, and head motion. All variables at each time point were covaried to adjust for shared variance. Non-significant paths ($ps > 0.1$) were removed one at a time within each model, and a chi-square difference test examined whether each removal significantly reduced model fit (order of removal and fit indices for the initial and final models are presented in the supplementary information). All stability paths were retained, even if non-significant, to adjust for baseline levels of each variable.

Effects of comorbid anxiety and medication

To ensure that group differences were not attributable to the presence of comorbid anxiety in the OCD group, we conducted ancillary between-group analyses on those edges for which group effects were detected across both FDR and NBS correction methods after excluding the OCD patients with comorbid anxiety. These ancillary analyses were conducted in IBM SPSS (v.23) using the multivariate analysis of variance command and, as in our initial whole-brain connectomic analyses, adjusted for age, sex, and head motion (i.e., mean FD). Rather than statistically adjusting for the presence of comorbid anxiety, these sensitivity analyses involved excluding participants because this variable was collinear with group (i.e., only participants in the OCD group had comorbid anxiety).

Similarly, for each cross-lagged panel model in which a significant relationship between functional connectivity and OCD symptoms pre- and post-CBT was detected, we conducted ancillary models: (1) adjusting for comorbid anxiety as a time varying covariate, and (2) excluding two patients who began taking SSRIs mid-treatment. Because these analyses were conducted in the OCD group only, the models adjusted for the

presence comorbid anxiety at each time point and did not require excluding participants from the analysis.

RESULTS

Participants

After quality control, rs-fMRI data were available from 25 OCD and 23 HC participants at baseline and from 21 OCD and 15 HC participants at follow-up (three patients and eight HC participants dropped out from treatment/study before completion). Demographic and clinical characteristics from the final sample are shown in Table 1. No significant baseline group differences in age, sex, or head motion were detected ($ps > 0.05$; Table 1). Among the 21 patients who completed the treatment protocol, total CY-BOCS scores declined significantly pre- to post-treatment ($t(20) = 6.230$, $p < 0.001$), with an average decrease of 9.3 ± 6.9 points ($38.6 \pm 16.4\%$). In all, 71% ($n = 15$) patients responded with >25% reduction in CY-BOCS and 52% ($N = 11$) with a >35% reduction. In all, 76% ($n = 16$) patients had a post-treatment CY-BOCS score ≤ 12.

Whole-brain connectome-level analyses

Functional connectivity findings are summarized in Fig. 2 and Table 2. Both FDR and NBS methods revealed significant group

Table 1. Participant demographics and clinical characteristics at baseline and follow-up.

Characteristics	Baseline			Follow-up		
	OCD ($n = 25$)	HC ($n = 23$)	Analysis[a]	OCD ($n = 21$)	HC ($n = 15$)	Analysis[a]
Age (years)	12.8 (2.9)	11.0 (3.3)	$t = 1.922$	12.2 (2.7)	11.9 (3.2)	$t = 0.327$
Sex (*n*/% female)	13 (52.0%)	12 (52.2%)	$\chi^2 = 0.00$	11 (52.4%)	8 (53.3%)	$\chi^2 = 0.00$
WASI-II IQ (full)	108.0 (16.7)	109.5 (12.1)	$t = -0.339$	111.2 (15.9)	113.4 (9.0)	$t = -0.518$
Head motion (FD)	0.03 (0.02)	0.05 (0.05)	$t = -1.628$	0.02 (0.01)	0.03 (0.02)	$t = -0.996$
CY-BOCS total	24.5 (5.2)	–	–	14.4 (6.5)	–	–
CY-BOCS obsession	11.9 (2.6)	–	–	7.3 (2.9)	–	–
CY-BOCS compulsion	12.6 (2.9)	–	–	7.1 (3.9)	–	–
CGI severity of illness	4.7 (0.7)	–	–	2.8 (1.0)	–	–

[a]No significant differences were detected (all $ps > 0.05$)
CGI Clinical Global Impressions scale, *CY-BOCS* Children's Yale-Brown Obsessive–Compulsive Scale, *FD* framewise displacement, *HC* healthy controls, *OCD* obsessive–compulsive disorder, *WAIS* Wechsler Abbreviated Scale of Intelligence—Second Edition

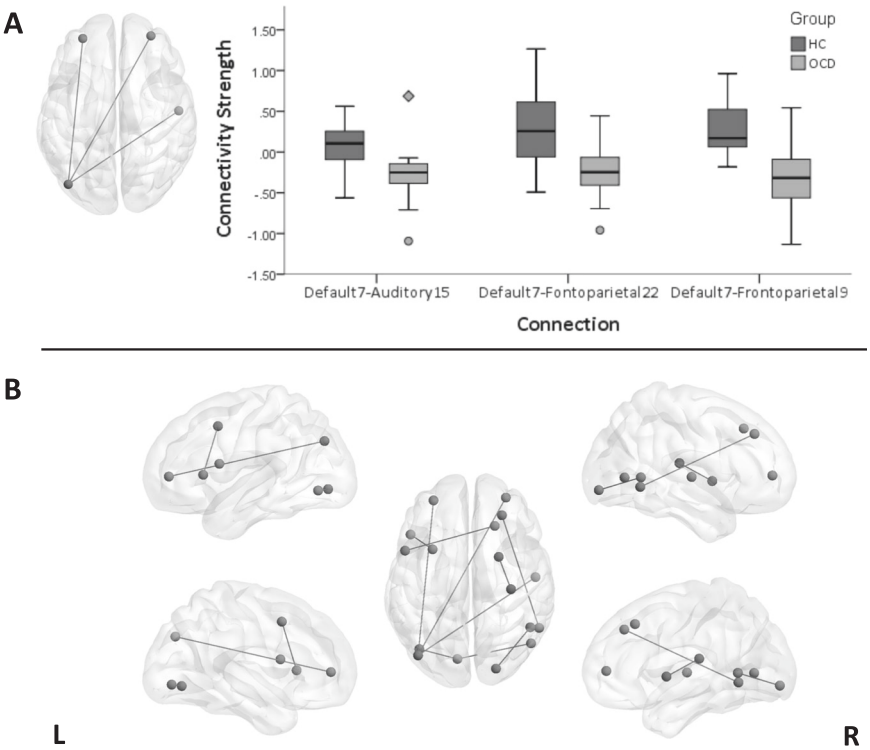

Fig. 2 Edges showing significant difference between participants with obsessive–compulsive disorder (OCD) and healthy controls (HC) in functional connectivity at baseline. a Significant edges according to both methods of correction for Type I error (i.e., false discovery rate (FDR) and network-based statistics (NBS)), along with boxplots displaying the distribution of connectivity strength (Fisher's *r*-to-*z* scores) in each group (circles on the boxplots indicate score > 1.5 × interquartile range [IQR] and diamonds indicate score > 3 × IQR). **b** Significant edges according to either correction method (i.e., FDR or NBS). Blue lines on brain overlays indicate HC > OCD and red color line indicates OCD > HC. The labels are based on the Cortical Area Parcellation from Resting-State Correlations data set (Gordon et al. [66]).

Table 2. Network connections that significantly differ between OCD ($N = 25$) and HC ($N = 23$) at baseline.

Contrast	Hemis	Label[a]	Region	BA	Hemis	Label[a]	Region	BA	*t*	*d*	Correction[b]
HC > OCD	Left	Default 7	Angular gyrus	BA39	Left	Frontoparietal 9	Rostral MFG	BA10	4.99	1.47	NBS, FDR
	Left	Default 7	Angular gyrus	BA39	Right	Frontoparietal 22	Rostral MFG	BA10	4.90	1.45	NBS, FDR
	Left	Default 7	Angular gyrus	BA39	Right	Auditory15	Posterior Insula	BA42	5.20	1.54	NBS, FDR
	Left	Default 19	Posterior MFG	BA8	Left	VentralAttn 5	IFG triangularis	BA45	4.69	1.38	FDR
	Right	Default 33	MFG	BA8	Left	CinguloOperc 18	IFG opercularis	BA44	4.31	1.27	FDR
	Right	Default 34	SFG	BA9	Right	DorsalAttn 30	Occipitotemporal	BA37	3.90	1.15	FDR
	Left	Visual 15	Medial occipital	BA18	Left	Visual 16	Occipitotemporal	BA37	4.02	1.19	FDR
	Left	Visual 15	Medial occipital	BA18	Right	Visual 29	Occipital	BA19	4.33	1.28	FDR
	Right	Visual 31	Occipitoparietal	BA39	Right	Visual 37	Occipital	BA19	4.10	1.21	FDR
OCD > HC	Right	Putamen	Putamen		Right	Auditory 13	Posterior Insula	BA42	4.49	1.33	FDR

[a]The labels are based on the Cortical Area Parcellation from Resting-State Correlations data set [66]
[b]Findings that survive false discovery rate (FDR) and network-based statistics (NBS) correction for multiple comparisons are reported. The first three rows show connections that survived both methods of correction
BA Broadmann Area, *FDR* false discovery rate, *HC* healthy controls, *Hemis* hemisphere, *IFG* inferior frontal gyrus, *MFG* middle frontal gyrus, *NBS* network-based statistics, *SFG* superior frontal gyrus, *OCD* obsessive–compulsive disorder

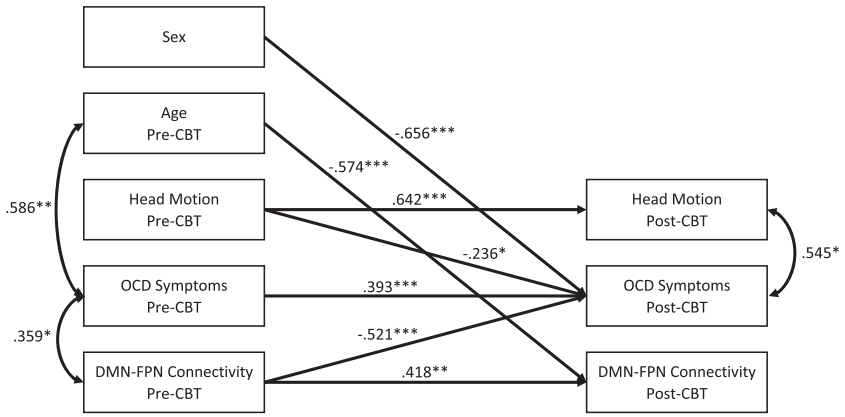

Fig. 3 Cross-lagged panel results relating obsessive–compulsive disorder (OCD) symptoms and functional connectivity before and after cognitive-behavioral therapy (CBT) treatment. *$p < 0.05$, **$p < 0.01$, ***$p < 0.001$. OCD symptoms are based on scores from the Children's Yale-Brown Obsessive–Compulsive Scale. Functional connectivity represents the Fisher's *r*-to-*z* scores between a default mode network (DMN) region (i.e., left angular gyrus; label *default 7*) and a frontoparietal network (FPN) region (i.e., left rostral middle frontal gyrus; label *frontoparietal 9*) based on the Cortical Area Parcellation from Resting-State Correlations dataset (Gordon et al. [66]). Regression parameters represent standardized estimates. Covariances between endogenous terms refer to covariances on the error terms of those variables. Values on covariances represent correlations.

differences in DMN-FPN and DMN-Auditory Network connectivity at baseline ($N = 25$ OCD and $N = 23$ HC). Specifically, relative to HC participants, patients with OCD exhibited reduced connectivity of left angular gyrus (parcel label *default 7*) with left and right rostral middle frontal gyrus (*frontoparietal 9* and *frontoparietal 22*), and with right posterior insula (*auditory 15*). In addition to these findings detected with both methods, the FDR method also yielded findings of reduced connectivity in patients with OCD between other DMN regions and "task-positive" network regions that are typically engaged during attention-demanding tasks (i.e., ventral and dorsal attention, and cingulo-opercular networks) [79–82], and between visual network regions (detailed in Table 2), as well as increased connectivity in OCD relative to HC participants was detected in between right putamen and posterior insula (part of the auditory network). No significant group-by-time interactions were detected with either FDR or NBS method ($Ns = 21$ OCD, 15 HC).

Cross-lagged panel modeling

Separate cross-lagged panel models were computed in the OCD group ($N = 25$) for the three edges that differed significantly across groups at baseline with both FDR and NBS (i.e., left angular gyrus (*default 7*) to left and right rostral middle frontal gyrus (*frontoparietal 9 and 22*), and to right posterior insula (*auditory15*)). Descriptive statistics and bivariate correlations between outcome variables are presented in Table S1. Figures 3 and S1 present the final models with significant connectivity-symptom associations pre- and post-CBT. Based on a Bonferroni correction for the three models tested, $ps < 0.017$ were considered significant and corrected. Greater (less reduced) left *default 7*-to-*frontoparietal 9* (DMN-to-left FPN) connectivity at baseline predicted greater reduction in OCD symptoms at follow-up ($B = -0.521$, $p < 0.001$; Fig. 3). In addition, less-severe OCD symptoms at baseline predicted greater increase in *default 7*-to-*Auditory 15* (left DMN-to-right auditory) connectivity at follow-up ($B = -0.580$, $p = 0.012$; Figure S2). In no instance did the removal of a non-significant path result in significant model fit reduction; thus, no non-significant path (other than stability paths) was retained in the final model. Detailed statistics and goodness of fit for the initial and final models are reported in the supplementary information and Table S2.

Effects of comorbid anxiety and medication

Baseline group differences in connectivity remained significant after excluding patients with comorbid anxiety ($F(3,24) = 8.473$, $p = 0.001$; $Ns = 8$ OCD, 23 HC). Relationships between functional connectivity and OCD symptoms pre- and post-CBT also remained significant after adjusting for comorbid anxiety in our cross-lagged panel models (Table S3; $N = 25$) and after excluding two patients who began receiving complementary SSRI medication mid-treatment (Table S4; $N = 23$).

DISCUSSION

Using a data-driven whole-brain connectomic approach, we identified altered functional connectivity between regions of canonical large-scale brain networks in pediatric OCD that also predicted response to CBT. Specifically, compared with their healthy counterparts, youth with OCD exhibited reduced connectivity between regions of the DMN and regions within several task-positive networks, including FPN, ventral attention, and cingulo-opercular. Increased connectivity between right putamen and posterior insula (auditory network) was also detected. In addition, *default 7*-to-*frontoparietal 9* connectivity at baseline associated inversely with OCD symptoms post-CBT, adjusting for baseline symptoms. These findings suggest that less-altered connectivity between these regions predicts better response to CBT in pediatric OCD.

Our findings of altered connectivity between task-positive and DMN regions are in line with meta-analytic findings showing consistent hypoconnectivity within and between FPN, salience, and DMN in adults and adolescents with OCD [47]. The salience network defined in that and other prior studies is comprised of insular cortex, ACC, supramarginal gyrus, and largely overlaps with the ventral attention and cingulo-opercular networks defined in the brain parcellation used herein [66]. Although these task-positive networks are comprised of regions engaged during goal-directed tasks requiring attention and cognitive control [79–82], DMN regions are typically engaged during rest [83–89], mind wandering, and self-referential processes [90–92]. Our findings of altered connectivity between task-positive and DMN regions may suggest a network imbalance, consistent with a triple network model [93], whereby the salience network interfaces between the DMN and FPN, acting like a switch modulating the attention and cognitive resources between self-referential thoughts, internal processes (i.e., DMN processes) and external goal-directed behavior (i.e., FPN processes). Imbalance across this triple network may underlie OCD [47], contributing to difficulty disengaging from obsessive thoughts and/or urges to perform compulsive behaviors in the service of more adaptive goal-directed behavior.

Cross-lagged panel modeling revealed that *default 7*-to-*frontoparietal 9* connectivity significantly predicted response to CBT, such that more (i.e., less reduced) connectivity was associated with greater reduction in OCD symptoms. Prior graph theory findings suggested reduced network segregation between the DMN and FPN in adults with OCD that normalized following SSRI treatment [54]. Although altered connectivity in the present study of children and adolescents did not normalize with CBT, both sets of findings suggest that altered DMN-FPN connectivity may mark the illness and serve as a target for symptom change. Other data from adults with OCD suggest that patterns of connectivity within the DMN significantly predicted response to CBT. Between-network connectivity was not assessed in that prior study, however, thereby precluding direct comparison between those findings and ours.

Previous findings from a small sample of youth with OCD ($N = 15$, 80% medicated) suggested reduced connectivity between left putamen and a cluster of regions in the salience/cingulo-opercular network, including a portion of the anterior insula [8]. In contrast, we detected increased connectivity between right putamen and right posterior insula, which is part of a different network (i.e., auditory). Findings from another small sample ($N = 14$) suggested increased connectivity between bilateral putamen and left-sided clusters encompassing posterior insula and surrounding cortical regions following SSRI treatment, with increased left putamen connectivity associated with clinical improvement [94]. Whereas these previous studies used a seed-based approach, we used a data-driven approach and rigorous correction methods—only exploring further those findings of group differences that survived both NBS and FDR corrections—precluding further comparison between these prior findings and ours. Nevertheless, these extant findings together suggest that network connectivity extending beyond CSTC circuits may be an important mediator or mechanism of symptom change, underscoring the clinical relevance of these networks as potential circuit-based targets for the development of novel treatments for pediatric OCD.

This is the first fMRI study to examine the effects of CBT on functional connectivity and relationships with symptom change in youth with OCD. Our data-driven connectomic approach permitted the identification of relevant markers that predict treatment response in large-scale brain networks, extending outside the classical CSTC circuits. We used stringent methods of multiple comparison correction to minimize the risk of type I error and carefully controlled for potential confounding effects, including age, sex, motion, and comorbid anxiety and SSRI augmentation in the OCD group, rendering our analyses quite conservative. Our cross-lagged panel models adjusted for the independent effects of these potential confounds as well as baseline levels of each predicted outcome variable (i.e., functional connectivity and OCD symptoms) in addition to the covariance between variables at each time point. These sophisticated longitudinal analyses thus allowed us to disentangle connectivity-symptom relationships pre- and post-CBT, thereby permitting inference about the directional influence of DMN-FPN connectivity on CBT-related change in OCD symptoms. Finally, all participants were medication-free and treatment-naive at baseline, received protocol driven CBT with excellent response, and potential effects of mid-treatment SSRI initiation in two patients were ruled out in ancillary analyses.

Notwithstanding these notable strengths, our modest sample size limited power to detect effects and precluded examining specific effects of, for example, different OCD symptom dimensions [95–97], comorbidities, or changes in functional connectivity pre-to-post CBT across the entire brain while preserving adequate stringency. As such, our study may have failed to detect several relevant effects that should be investigated in future multi-site studies of much larger pediatric OCD samples. Relatedly, altered connectivity at baseline in the OCD relative to HC participants did not significantly normalize with CBT, as suggested by our lack of group-by-time interactions in our whole-brain connectomic analyses. However, these findings should be interpreted with caution given the modest number of HC participants with follow-up data ($N = 15$ HC), which rendered these analyses underpowered to detect effects. Inclusion of OCD participants with comorbid anxiety disorders is another limitation, however exploratory analyses revealed that this comorbidity did not contribute to our findings of altered connectivity and its prediction of CBT response in pediatric OCD. Although we employed a longitudinal design that permitted the examination of the directionality of relationships between symptoms and functional connectivity pre- and post-CBT, the collection of symptom and connectivity data along more time points would have allowed examination of how connectivity predicts long-term remission or relapse. Another limitation is that there was no placebo control group (e.g., OCD patients undergoing relaxation therapy) or a waitlist group. It may be that the relationships between functional connectivity and symptom change were not specific to CBT per se. Finally, a

limitation inherent to our connectomic approach is the lack of any gold standard for large-scale brain parcellation, resulting in node definition being somewhat arbitrary and inconsistent across studies [77]. All available parcellation methods have respective advantages and limitations: coarser parcellations typically comprise functionally heterogeneous regions and may fail to detect true effects. Alternatively, finer parcellations (e.g., treating each voxel as a separate node) may fail to account for the large homogeneity across neighboring nodes and result in noisy and underpowered estimates. In the present study, we used a parcellation scheme developed based on the recent technological advances in MRI acquisition, with greater parcel homogeneity than alternative parcellations and reliable mapping of known architectonic areas and connectivity patterns across individual participants [66].

In conclusion, this study is first to employ a data-driven whole-brain connectomic approach to examine network connectivity in pediatric OCD before and after a full course of CBT treatment. Our innovative analytical approach combined with high temporal resolution fMRI data allowed to identify abnormalities between networks that extend outside the classical CSTC circuits. Cross-lagged panel modeling of longitudinal data allowed to disentangle the directionality of the relationships between functional connectivity and OCD symptoms in response to CBT. Our findings point to altered task-positive and task-negative networks connectivity in pediatric OCD that may play a key role in patient's ability to benefit from CBT. Future longitudinal studies of large samples should replicate and extend these findings that may ultimately lead to treatment targets for future circuit-based interventions.

FUNDING AND DISCLOSURE

This work was supported by a grant from the National Institute of Mental Health (R21MH101441; MPIs: Marsh and Rynn) and by a fellowship from the Fonds de Recherche du Quebec, Sante (Fellow: Cyr). The study was registered with clinicaltrials.gov (NCT02421315). Dr. Moira Rynn receives an honorarium as a DSMB member from Allergan Inc. All other authors declare no competing interests.

ADDITIONAL INFORMATION

Supplementary Information accompanies this paper at (https://doi.org/10.1038/s41386-020-0613-3).

Publisher's note Springer Nature remains neutral with regard to jurisdictional claims in published maps and institutional affiliations.

REFERENCES

1. Vaghi MM, Vertes PE, Kitzbichler MG, Apergis-Schoute AM, van der Flier FE, Fineberg NA, et al. Specific frontostriatal circuits for impaired cognitive flexibility and goal-directed planning in obsessive-compulsive disorder: evidence from resting-state functional connectivity. Biol Psychiatry 2017;81:708–17.
2. Sakai Y, Narumoto J, Nishida S, Nakamae T, Yamada K, Nishimura T, et al. Corticostriatal functional connectivity in non-medicated patients with obsessive-compulsive disorder. Eur Psychiatry 2011;26:463–9.
3. Posner J, Marsh R, Maia TV, Peterson BS, Gruber A, Simpson HB. Reduced functional connectivity within the limbic cortico-striato-thalamo-cortical loop in unmedicated adults with obsessive-compulsive disorder. Hum Brain Mapp. 2014;35:2852–60.
4. Ping L, Su-Fang L, Hai-Ying H, Zhang-Ye D, Jia L, Zhi-Hua G, et al. Abnormal spontaneous neural activity in obsessive-compulsive disorder: a resting-state functional magnetic resonance imaging study. PLoS ONE 2013;8:e67262.
5. Jung WH, Kang DH, Kim E, Shin KS, Jang JH, Kwon JS. Abnormal corticostriatal-limbic functional connectivity in obsessive-compulsive disorder during reward processing and resting-state. NeuroImage Clin. 2013;3:27–38.
6. Harrison BJ, Soriano-Mas C, Pujol J, Ortiz H, Lopez-Sola M, Hernandez-Ribas R, et al. Altered corticostriatal functional connectivity in obsessive-compulsive disorder. Arch Gen Psychiatry. 2009;66:1189–200.
7. Beucke JC, Sepulcre J, Talukdar T, Linnman C, Zschenderlein K, Endrass T, et al. Abnormally high degree connectivity of the orbitofrontal cortex in obsessive-compulsive disorder. JAMA Psychiatry 2013;70:619–29.
8. Bernstein GA, Mueller BA, Schreiner MW, Campbell SM, Regan EK, Nelson PM, et al. Abnormal striatal resting-state functional connectivity in adolescents with obsessive-compulsive disorder. Psychiatry Res Neuroimaging. 2016;247:49–56.
9. Abe Y, Sakai Y, Nishida S, Nakamae T, Yamada K, Fukui K, et al. Hyper-influence of the orbitofrontal cortex over the ventral striatum in obsessive-compulsive disorder. Eur Neuropsychopharmacol 2015;25:1898–905.
10. Takagi Y, Sakai Y, Lisi G, Yahata N, Abe Y, Nishida S, et al. A neural marker of obsessive-compulsive disorder from whole-brain functional connectivity. Sci Rep. 2017;7:7538.
11. Menzies L, Chamberlain SR, Laird AR, Thelen SM, Sahakian BJ, Bullmore ET. Integrating evidence from neuroimaging and neuropsychological studies of obsessive-compulsive disorder: the orbitofronto-striatal model revisited. Neurosci Biobehav Rev. 2008;32:525–49.
12. Anticevic A, Hu S, Zhang S, Savic A, Billingslea E, Wasylink S, et al. Global resting-state functional magnetic resonance imaging analysis identifies frontal cortex, striatal, and cerebellar dysconnectivity in obsessive-compulsive disorder. Biol Psychiatry 2014;75:595–605.
13. Beucke JC, Sepulcre J, Eldaief MC, Sebold M, Kathmann N, Kaufmann C. Default mode network subsystem alterations in obsessive-compulsive disorder. Br J Psychiatry. 2014;205:376–82.
14. Goncalves OF, Soares JM, Carvalho S, Leite J, Ganho-Avila A, Fernandes-Goncalves A, et al. Patterns of default mode network deactivation in obsessive compulsive disorder. Sci Rep. 2017;7:44468.
15. Hou JM, Zhao M, Zhang W, Song LH, Wu WJ, Wang J, et al. Resting-state functional connectivity abnormalities in patients with obsessive-compulsive disorder and their healthy first-degree relatives. J Psychiatry Neurosci. 2014;39:304–11.
16. Posner J, Song I, Lee S, Rodriguez CI, Moore H, Marsh R, et al. Increased functional connectivity between the default mode and salience networks in unmedicated adults with obsessive-compulsive disorder. Hum Brain Mapp. 2017;38:678–87.
17. Stern ER, Fitzgerald KD, Welsh RC, Abelson JL, Taylor SF. Resting-state functional connectivity between fronto-parietal and default mode networks in obsessive-compulsive disorder. PLoS ONE 2012;7:e36356.
18. Tian L, Meng C, Jiang Y, Tang Q, Wang S, Xie X, et al. Abnormal functional connectivity of brain network hubs associated with symptom severity in treatment-naive patients with obsessive-compulsive disorder: a resting-state functional MRI study. Prog Neuropsychopharmacol Biol Psychiatry. 2016;66:104–11.
19. Zhu Y, Fan Q, Zhang H, Qiu J, Tan L, Xiao Z, et al. Altered intrinsic insular activity predicts symptom severity in unmedicated obsessive-compulsive disorder patients: a resting state functional magnetic resonance imaging study. BMC Psychiatry 2016;16:104.
20. Armstrong CC, Moody TD, Feusner JD, McCracken JT, Chang S, Levitt JG, et al. Graph-theoretical analysis of resting-state fMRI in pediatric obsessive-compulsive disorder. J Affect Disord. 2016;193:175–84.
21. Chen Y, Meng X, Hu Q, Cui H, Ding Y, Kang L, et al. Altered resting-state functional organization within the central executive network in obsessive-compulsive disorder. Psychiatry Clin Neurosci. 2016;70:448–56.
22. Ost LG, Havnen A, Hansen B, Kvale G. Cognitive behavioral treatments of obsessive-compulsive disorder. A systematic review and meta-analysis of studies published 1993-2014. Clin Psychol Rev. 2015;40:156–69.
23. Rosa-Alcazar AI, Sanchez-Meca J, Gomez-Conesa A, Marin-Martinez F. Psychological treatment of obsessive-compulsive disorder: a meta-analysis. Clin Psychol Rev. 2008;28:1310–25.
24. Rosa-Alcazar AI, Sanchez-Meca J, Rosa-Alcazar A, Iniesta-Sepulveda M, Olivares-Rodriguez J, Parada-Navas JL. Psychological treatment of obsessive-compulsive disorder in children and adolescents: a meta-analysis. Span J Psychol. 2015;18:E20.
25. Simpson HB, Liebowitz MR, Foa EB, Kozak MJ, Schmidt AB, Rowan V, et al. Post-treatment effects of exposure therapy and clomipramine in obsessive-compulsive disorder. Depress Anxiety 2004;19:225–33.
26. Abramowitz JS, Whiteside SP, Deacon BJ. The effectiveness of treatment for pediatric obsessive-compulsive disorder: a meta-analysis. Behav Ther 2005;36:55–63.
27. Ost LG, Riise EN, Wergeland GJ, Hansen B, Kvale G. Cognitive behavioral and pharmacological treatments of OCD in children: a systematic review and meta-analysis. J Anxiety Disord. 2016;43:58–69.
28. Watson HJ, Rees CS. Meta-analysis of randomized, controlled treatment trials for pediatric obsessive-compulsive disorder. J Child Psychol Psychiatry Allied Discip. 2008;49:489–98.
29. Abramowitz JS. The psychological treatment of obsessive-compulsive disorder. Can J Psychiatry. 2006;51:407–16.
30. Franklin ME, Sapyta J, Freeman JB, Khanna M, Compton S, Almirall D, et al. Cognitive behavior therapy augmentation of pharmacotherapy in pediatric

obsessive-compulsive disorder: the Pediatric OCD Treatment Study II (POTS II) randomized controlled trial. JAMA 2011;306:1224–32.
31. Olatunji BO, Ferreira-Garcia R, Caseras X, Fullana MA, Wooderson S, Speckens A, et al. Predicting response to cognitive behavioral therapy in contamination-based obsessive-compulsive disorder from functional magnetic resonance imaging. Psychological Med 2014;44:2125–37.
32. Pediatric OCDTST. Cognitive-behavior therapy, sertraline, and their combination for children and adolescents with obsessive-compulsive disorder: the Pediatric OCD Treatment Study (POTS) randomized controlled trial. JAMA 2004;292: 1969–76.
33. Milad MR, Rauch SL. Obsessive-compulsive disorder: beyond segregated cortico-striatal pathways. Trends Cogn Sci. 2012;16:43–51.
34. Pauls DL, Abramovitch A, Rauch SL, Geller DA. Obsessive-compulsive disorder: an integrative genetic and neurobiological perspective. Nat Rev Neurosci. 2014;15:410–24.
35. Saxena S, Rauch SL. Functional neuroimaging and the neuroanatomy of obsessive-compulsive disorder. Psychiatr Clin North Am. 2000;23:563–86.
36. Admon R, Bleich-Cohen M, Weizmant R, Poyurovsky M, Faragian S, Hendler T. Functional and structural neural indices of risk aversion in obsessive-compulsive disorder (OCD). Psychiatry Res 2012;203:207–13.
37. Boedhoe PS, Schmaal L, Abe Y, Ameis SH, Arnold PD, Batistuzzo MC, et al. Distinct subcortical volume alterations in pediatric and adult OCD: a worldwide meta- and mega-analysis. Am J Psychiatry. 2017;174:60–69.
38. Boedhoe PSW, Schmaal L, Abe Y, Alonso P, Ameis SH, Anticevic A, et al. Cortical abnormalities associated with pediatric and adult obsessive-compulsive disorder: findings from the ENIGMA Obsessive-Compulsive Disorder Working Group. Am J Psychiatry. 2018;175:453–62.
39. de Wit SJ, Alonso P, Schweren L, Mataix-Cols D, Lochner C, Menchon JM, et al. Multicenter voxel-based morphometry mega-analysis of structural brain scans in obsessive-compulsive disorder. Am J Psychiatry. 2014;171:340–9.
40. He X, Steinberg E, Stefan M, Fontaine M, Simpson HB, Marsh R. Altered frontal interhemispheric and fronto-limbic structural connectivity in unmedicated adults with obsessive-compulsive disorder. Hum Brain Mapp. 2018;39:803–10.
41. Hu X, Liu Q, Li B, Tang W, Sun H, Li F, et al. Multivariate pattern analysis of obsessive-compulsive disorder using structural neuroanatomy. Eur Neuropsychopharmacol 2016;26:246–54.
42. Li F, Huang X, Tang W, Yang Y, Li B, Kemp GJ, et al. Multivariate pattern analysis of DTI reveals differential white matter in individuals with obsessive-compulsive disorder. Hum Brain Mapp. 2014;35:2643–51.
43. Marsh R, Horga G, Parashar N, Wang Z, Peterson BS, Simpson HB. Altered activation in fronto-striatal circuits during sequential processing of conflict in unmedicated adults with obsessive-compulsive disorder. Biol Psychiatry 2014;75:615–22.
44. Nakamae T, Sakai Y, Abe Y, Nishida S, Fukui K, Yamada K, et al. Altered fronto-striatal fiber topography and connectivity in obsessive-compulsive disorder. PLoS ONE 2014;9:e112075.
45. Rotge JY, Guehl D, Dilharreguy B, Cuny E, Tignol J, Bioulac B, et al. Provocation of obsessive-compulsive symptoms: a quantitative voxel-based meta-analysis of functional neuroimaging studies. J Psychiatry Neurosci. 2008;33:405–12.
46. Soriano-Mas C, Pujol J, Alonso P, Cardoner N, Menchon JM, Harrison BJ, et al. Identifying patients with obsessive-compulsive disorder using whole-brain anatomy. Neuroimage 2007;35:1028–37.
47. Gursel DA, Avram M, Sorg C, Brandl F, Koch K. Frontoparietal areas link impairments of large-scale intrinsic brain networks with aberrant fronto-striatal interactions in OCD: a meta-analysis of resting-state functional connectivity. Neurosci Biobehav Rev. 2018;87:151–60.
48. Feusner JD, Moody T, Lai TM, Sheen C, Khalsa S, Brown J, et al. Brain connectivity and prediction of relapse after cognitive-behavioral therapy in obsessive-compulsive disorder. Front Psychiatry 2015;6:74.
49. Gottlich M, Kramer UM, Kordon A, Hohagen F, Zurowski B. Resting-state connectivity of the amygdala predicts response to cognitive behavioral therapy in obsessive compulsive disorder. Biol Psychol 2015;111:100–9.
50. Gruner P, Vo A, Argyelan M, Ikuta T, Degnan AJ, John M, et al. Independent component analysis of resting state activity in pediatric obsessive-compulsive disorder. Hum Brain Mapp. 2014;35:5306–15.
51. Meunier D, Ersche KD, Craig KJ, Fornito A, Merlo-Pich E, Fineberg NA, et al. Brain functional connectivity in stimulant drug dependence and obsessive-compulsive disorder. Neuroimage 2012;59:1461–8.
52. Moody TD, Morfini F, Cheng G, Sheen C, Tadayonnejad R, Reggente N, et al. Mechanisms of cognitive-behavioral therapy for obsessive-compulsive disorder involve robust and extensive increases in brain network connectivity. Transl Psychiatry 2017;7:e1230.
53. Reggente N, Moody TD, Morfini F, Sheen C, Rissman J, O'Neill J, et al. Multivariate resting-state functional connectivity predicts response to cognitive behavioral therapy in obsessive-compulsive disorder. Proc Natl Acad Sci USA. 2018;115:2222–27.
54. Shin DJ, Jung WH, He Y, Wang J, Shim G, Byun MS, et al. The effects of pharmacological treatment on functional brain connectome in obsessive-compulsive disorder. Biol Psychiatry 2014;75:606–14.
55. Zhang T, Wang J, Yang Y, Wu Q, Li B, Chen L, et al. Abnormal small-world architecture of top-down control networks in obsessive-compulsive disorder. J Psychiatry Neurosci. 2011;36:23–31.
56. Morgieve M, N'Diaye K, Haynes WI, Granger B, Clair AH, Pelissolo A, et al. Dynamics of psychotherapy-related cerebral haemodynamic changes in obsessive compulsive disorder using a personalized exposure task in functional magnetic resonance imaging. Psychological Med 2014;44:1461–73.
57. Nabeyama M, Nakagawa A, Yoshiura T, Nakao T, Nakatani E, Togao O, et al. Functional MRI study of brain activation alterations in patients with obsessive-compulsive disorder after symptom improvement. Psychiatry Res 2008;163: 236–47.
58. Nakao T, Nakagawa A, Yoshiura T, Nakatani E, Nabeyama M, Yoshizato C, et al. Brain activation of patients with obsessive-compulsive disorder during neuropsychological and symptom provocation tasks before and after symptom improvement: a functional magnetic resonance imaging study. Biol Psychiatry 2005;57:901–10.
59. Yang XY, Sun J, Luo J, Zhong ZX, Li P, Yao SM, et al. Regional homogeneity of spontaneous brain activity in adult patients with obsessive-compulsive disorder before and after cognitive behavioural therapy. J Affect Disord. 2015;188:243–51.
60. Cole DA, Maxwell SE. Testing mediational models with longitudinal data: questions and tips in the use of structural equation modeling. J Abnorm Psychol. 2003;112:558–77.
61. Jöreskog KG. A general method for estimating a linear structural equation system. In: Goldberger AS, Duncan OD, (eds.) Structural equation models in the social sciences. New York: Seminar Press; 1973. p 255–84.
62. Jöreskog KG, Sörbom D, Magidson J. Advances in factor analysis and structural equation models. New York: University Press of America; 1979.
63. Cyr M, Fontaine M, Stefan M, Terranova K, Kopala-Sibley DC, Attia E, et al. A longitudinal functional magnetic resonance imaging study of task control circuits and bulimic symptoms over adolescence. J Child Psychol Psychiatry Allied Discip. 2018;59:752–62.
64. Allen M. Cross-Lagged Panel Analysis. The SAGE Encyclopedia of Communication Research Methods. 2017.
65. Finkel SE. Causal analysis with panel data. Thousand Oaks, CA: Sage Publications, Inc; 1995.
66. Gordon EM, Laumann TO, Adeyemo B, Huckins JF, Kelley WM, Petersen SE. Generation and evaluation of a cortical area parcellation from resting-state correlations. Cereb Cortex 2016;26:288–303.
67. Power JD, Schlaggar BL, Petersen SE. Studying brain organization via spontaneous fMRI signal. Neuron 2014;84:681–96.
68. Albano AM, Siverman WK. The anxiety disorders interview schedule for DSM-5-child and parent versions. New York: Oxford University Press; in Press.
69. Wechsler D. Wechsler abbreviated scale of intelligence. San Antonio, TX: The Psychological Corporation; 1999.
70. Riddle MA, Scahill L, King RA, Hardin MT, Anderson GM, Ort SI, et al. Double-blind, crossover trial of fluoxetine and placebo in children and adolescents with obsessive-compulsive disorder. J Am Acad Child Adolesc Psychiatry. 1992;31:1062–9.
71. Scahill L, Riddle MA, McSwiggin-Hardin M, Ort SI, King RA, Goodman WK, et al. Children's Yale-Brown Obsessive Compulsive Scale: reliability and validity. J Am Acad Child Adolesc Psychiatry. 1997;36:844–52.
72. Guy W Clinical Global Impressions. ECDEU Assessment Manual for Psychopharmacology-Revised. Rcokville, MD: U.S. Department of Health, Education, and Welfare, Public Health Service, Alcohol, Drug Abuse, and Mental Health Administration, NIMH Psychopharmacology Branch, Division of Extramural Research Programs, Washington, DC; 1976.
73. March JS, Mulle K. OCD in children and adolescents: a cognitive-behavioral treatment manual. 1st ed. New York: The Guilford Press; 1998.
74. Van Essen DC, Ugurbil K, Auerbach E, Barch D, Behrens TE, Bucholz R, et al. The Human Connectome Project: a data acquisition perspective. Neuroimage 2012;62:2222–31.
75. Glasser MF, Sotiropoulos SN, Wilson JA, Coalson TS, Fischl B, Andersson JL, et al. The minimal preprocessing pipelines for the Human Connectome Project. Neuroimage 2013;80:105–24.
76. Fischl B, Salat DH, Busa E, Albert M, Dieterich M, Haselgrove C, et al. Whole brain segmentation: automated labeling of neuroanatomical structures in the human brain. Neuron 2002;33:341–55.
77. Zalesky A, Fornito A, Bullmore ET. Network-based statistic: identifying differences in brain networks. Neuroimage 2010;53:1197–207.
78. Finkel SE. Causal analysis with panel data. Beverly Hills: Sage Publications; 1995.
79. Curtis CE, D'Esposito M. Persistent activity in the prefrontal cortex during working memory. Trends Cogn Sci. 2003;7:415–23.

80. Kerns JG, Cohen JD, MacDonald AW 3rd, Cho RY, Stenger VA, Carter CS. Anterior cingulate conflict monitoring and adjustments in control. Science. 2004;303: 1023–6.
81. Menon V, Adleman NE, White CD, Glover GH, Reiss AL. Error-related brain activation during a Go/NoGo response inhibition task. Hum Brain Mapp. 2001;12:131–43.
82. Ridderinkhof KR, Ullsperger M, Crone EA, Nieuwenhuis S. The role of the medial frontal cortex in cognitive control. Science. 2004;306:443–7.
83. Beckmann CF, DeLuca M, Devlin JT, Smith SM. Investigations into resting-state connectivity using independent component analysis. Philos Trans R Soc Lond B Biol Sci. 2005;360:1001–13.
84. Biswal B, Yetkin FZ, Haughton VM, Hyde JS. Functional connectivity in the motor cortex of resting human brain using echo-planar MRI. Magn Reson Med. 1995;34:537–41.
85. Biswal BB, Van Kylen J, Hyde JS. Simultaneous assessment of flow and BOLD signals in resting-state functional connectivity maps. NMR Biomed 1997;10:165–70.
86. Fox MD, Snyder AZ, Vincent JL, Corbetta M, Van Essen DC, Raichle ME. The human brain is intrinsically organized into dynamic, anticorrelated functional networks. Proc Natl Acad Sci USA. 2005;102:9673–8.
87. Greicius MD, Krasnow B, Reiss AL, Menon V. Functional connectivity in the resting brain: a network analysis of the default mode hypothesis. Proc Natl Acad Sci USA. 2003;100:253–8.
88. Raichle ME, MacLeod AM, Snyder AZ, Powers WJ, Gusnard DA, Shulman GL. A default mode of brain function. Proc Natl Acad Sci USA. 2001;98:676–82.
89. Shulman GL, Fiez JA, Corbetta M, Buckner RL, Miezin FM, Raichle ME, et al. Common blood flow changes across visual tasks: ii. decreases in cerebral cortex. J Cogn Neurosci. 1997;9:648–63.
90. Harrison BJ, Pujol J, Lopez-Sola M, Hernandez-Ribas R, Deus J, Ortiz H, et al. Consistency and functional specialization in the default mode brain network. Proc Natl Acad Sci USA. 2008;105:9781–6.
91. Mason MF, Norton MI, Van Horn JD, Wegner DM, Grafton ST, Macrae CN. Wandering minds: the default network and stimulus-independent thought. Science 2007;315:393–5.
92. McKiernan KA, D'Angelo BR, Kaufman JN, Binder JR. Interrupting the "stream of consciousness": an fMRI investigation. Neuroimage 2006;29:1185–91.
93. Menon V. Large-scale brain networks and psychopathology: a unifying triple network model. Trends Cogn Sci. 2011;15:483–506.
94. Bernstein GA, Cullen KR, Harris EC, Conelea CA, Zagoloff AD, Carstedt PA, et al. Sertraline effects on striatal resting-state functional connectivity in youth with OCD: a pilot study. J Am Acad Child Adolesc Psychiatry. 2019;58:486–495.
95. Abramowitz JS, Deacon BJ, Olatunji BO, Wheaton MG, Berman NC, Losardo D, et al. Assessment of obsessive-compulsive symptom dimensions: development and evaluation of the dimensional obsessive-compulsive scale. Psychol Assess 2010;22:180–98.
96. Mataix-Cols D, Rosario-Campos MC, Leckman JF. A multidimensional model of obsessive-compulsive disorder. Am J Psychiatry. 2005;162:228–38.
97. McKay D, Abramowitz JS, Calamari JE, Kyrios M, Radomsky A, Sookman D, et al. A critical evaluation of obsessive-compulsive disorder subtypes: symptoms versus mechanisms. Clin Psychol Rev. 2004;24:283–313.